Title: Spike-based functional connectivity in cerebral cortex and hippocampus: loss of global connectivity is coupled to preservation of local connectivity during non-REM sleep.

Abbreviated title: Brain-state modulation of neuron-level coupling

Authors: Umberto Olcese*, Jeroen J. Bos*, Martin Vinck*, Jan V. Lankelma, Laura B. van Mourik-Donga, Friederike Schlumm, Cyriel M.A. Pennartz

Additional footnotes: *: these authors contributed equally to this study

Affiliations: Cognitive and Systems Neuroscience Group, Swammerdam Institute for Life Sciences, University of Amsterdam, Science Park 904, 1098XH Amsterdam, The Netherlands

Corresponding author: Cyriel M.A. Pennartz, c.m.a.pennartz@uva.nl, Cognitive and Systems Neuroscience Group, Swammerdam Institute for Life Sciences, University of Amsterdam, Science Park 904, 1098XH Amsterdam, The Netherlands

Supplemental online-only material

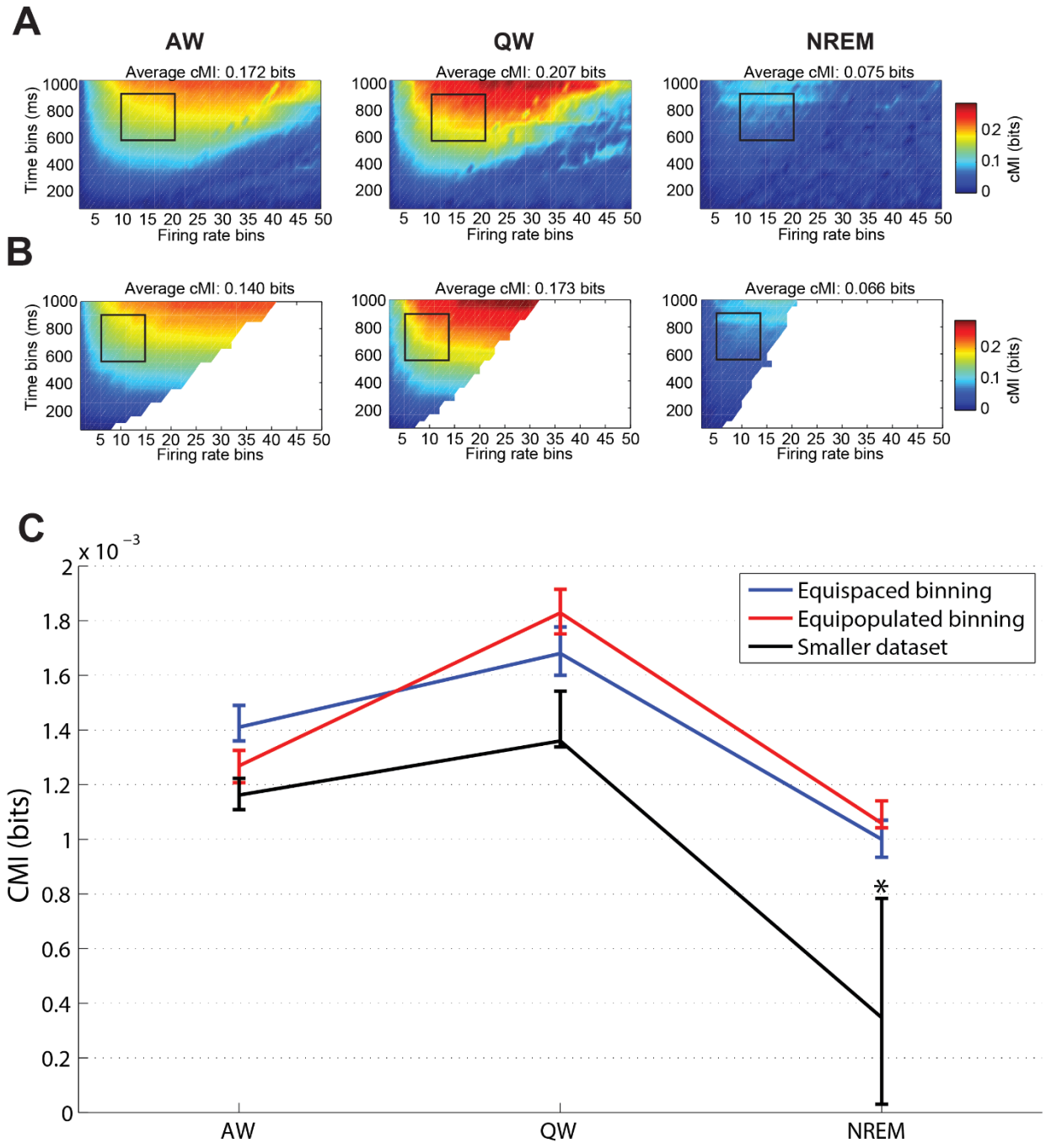

Figure R1 – Comparison of binning methods and evaluation of debiasing procedure. A. *Values of cMI for an example pair of neurons, computed using equispaced amplitude binning. Each plot corresponds to one behavioral state. cMI has been computed for time bins of different durations (y axis, 50 to 1000 ms with a step size of 50 ms) and for different amplitude bins (x axis, 2 to 50 bins). The black outline indicates the time bins and amplitude bins that were used in all further analyses. (Same as Fig. 2A).The average cMI value in for bins within the black outline is indicated in the header of each subplot.* ***B.*** *Same as A, but using equipopulated amplitude binning. Note the high similarity between cMI values computed with the two different binning procedures.* ***C.*** *Median cMI values for all connections as a function of brain state. Blue: values computed using equispaced amplitude binning. Red: values computed using equipopulated amplitude binning. Black: values computed using equispaced amplitude binning, and only 50% of (randomly selected) epochs for each recording session. Error bars indicate confidence intervals*

for the medians. The black asterisk indicates that, during NREM, estimates obtained using the smaller dataset were significantly lower (p=0.03) than those obtained with the complete dataset.

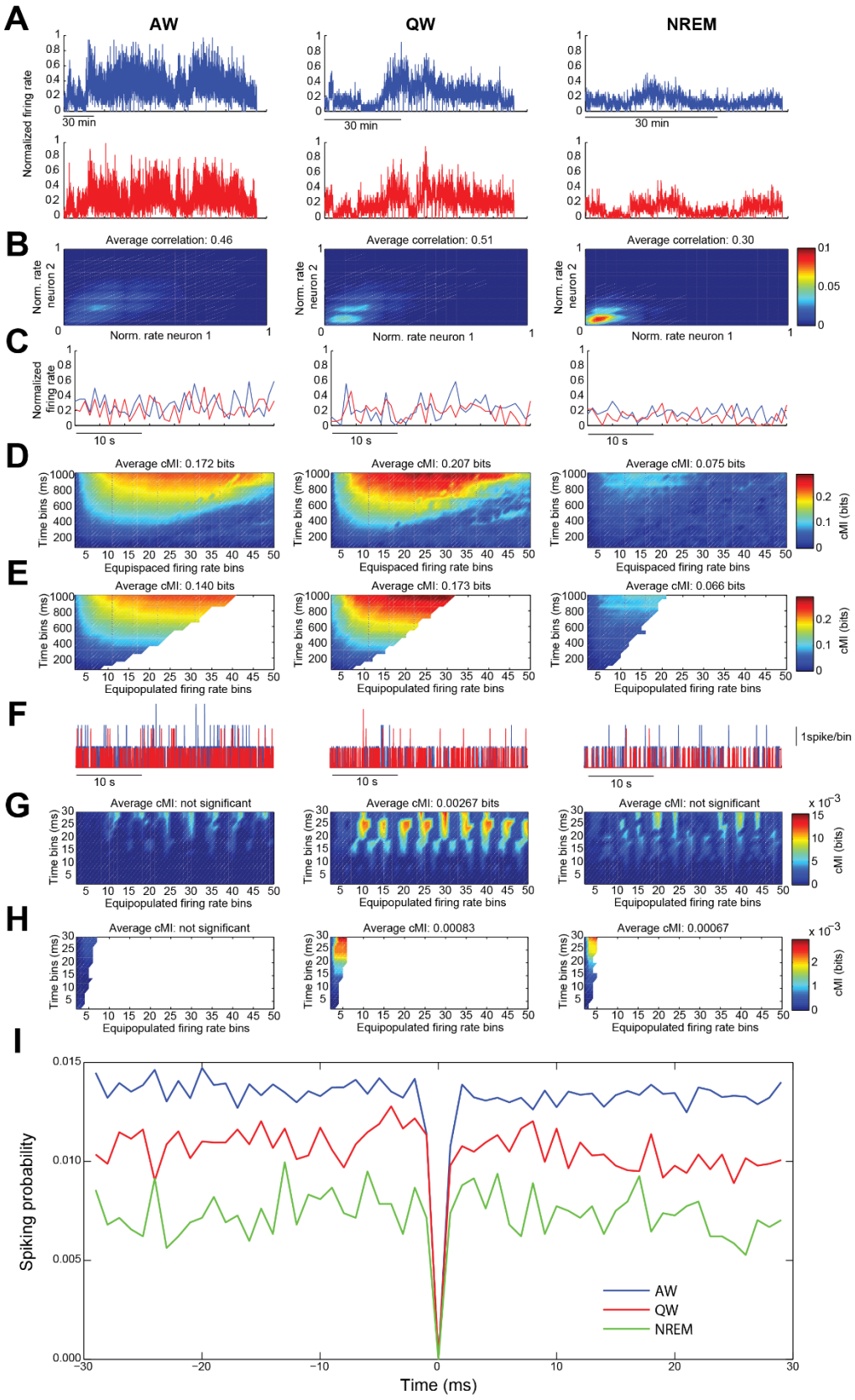
A
AW
QW
NREM
Normalized firing rate
30 min
B
Average correlation: 0.46
Average correlation: 0.51
Average correlation: 0.30
Norm. rate neuron 2
Norm. rate neuron 1
C
Normalized firing rate
10 s
D
Average cMI: 0.172 bits
Average cMI: 0.207 bits
Average cMI: 0.075 bits
Time bins (ms)
Equipispaced firing rate bins
Equispaced firing rate bins
Equispaced firing rate bins
cMI (bits)
E
Average cMI: 0.140 bits
Average cMI: 0.173 bits
Average cMI: 0.066 bits
Equipopulated firing rate bins
F
1spike/bin
G
Average cMI: not significant
Average cMI: 0.00267 bits
Average cMI: not significant
x 10^-3
H
Average cMI: not significant
Average cMI: 0.00083
Average cMI: 0.00067
I
Spiking probability
Time (ms)
AW
QW
NREM

Figure R2 - Example neuronal pair and related cMI values at different temporal scales. A. *Example normalized firing rates (800 ms bin) for two example neurons (blue and red traces), across the three brain states (left: AW, middle: QW, right: NREM). All epochs classified as either AW, QW or NREM have been collapsed (i.e. drawn adjacent to each other). Firing rates for each neuron have been normalized to the highest firing rate recorded across all brain states.* ***B****. Joint probability distribution plot for the normalized firing rates of the two example neurons, for each brain state. For visualization purposes, time bins in which the two neurons did not fire any action potential were excluded from these plots. The correlation value between the firing rates of the two neurons, computed in each brain state, is indicated in the header of each plot.* ***C.*** *Enlargement of the firing rate traces shown in A.* ***D.*** *cMI values for the example neuronal pair, computed using equispaced amplitude binning, as a function of brain state, number of amplitude bins and temporal bin duration. The average cMI value in the interval used in all the analyses of this study is indicated in the header of each subplot.* ***E.*** *Same as D, but using equipopulated amplitude binning.* ***F.*** *Same as C (the very same intervals are plotted here) computed using a 20 ms time bin.* ***G.*** *Same as D, for time bins ranging from 2 ms to 30 ms. Average cMI values have been computed over the 2-30 ms time interval.* ***H.*** *Same as G, using equipopulated amplitude binning. I. Cross-correlograms (probability of one spike in neuron A being followed or preceded by a spike in neuron B) for the example neuronal pair in the range -30 ms to 30 ms, for each brain state (blue: AW, red: QW, green: NREM).*

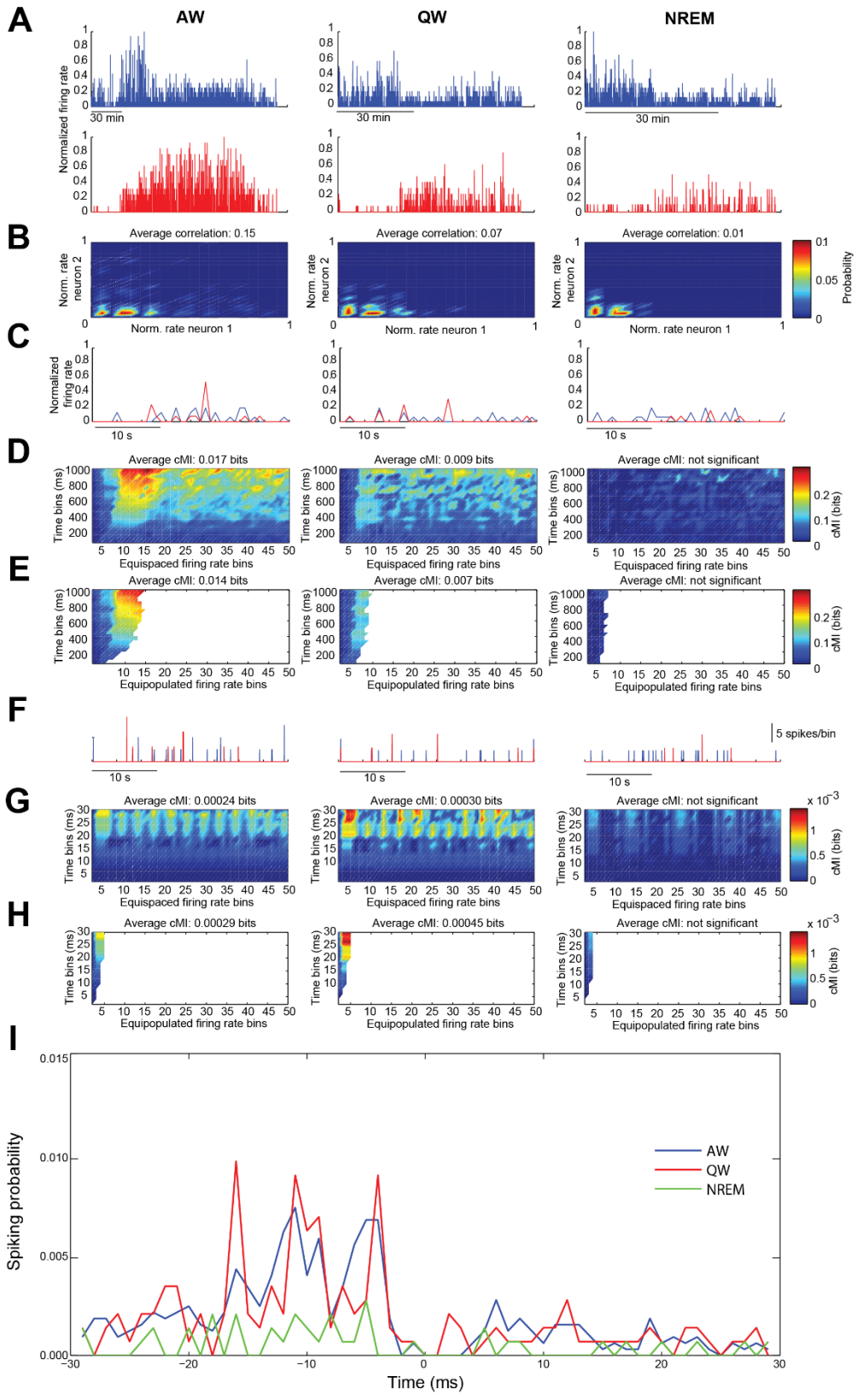

Figure R3 - Example neuronal pair and related cMI values at different temporal scales. All panels: *Same as R2, but for a different pair of example neurons.*

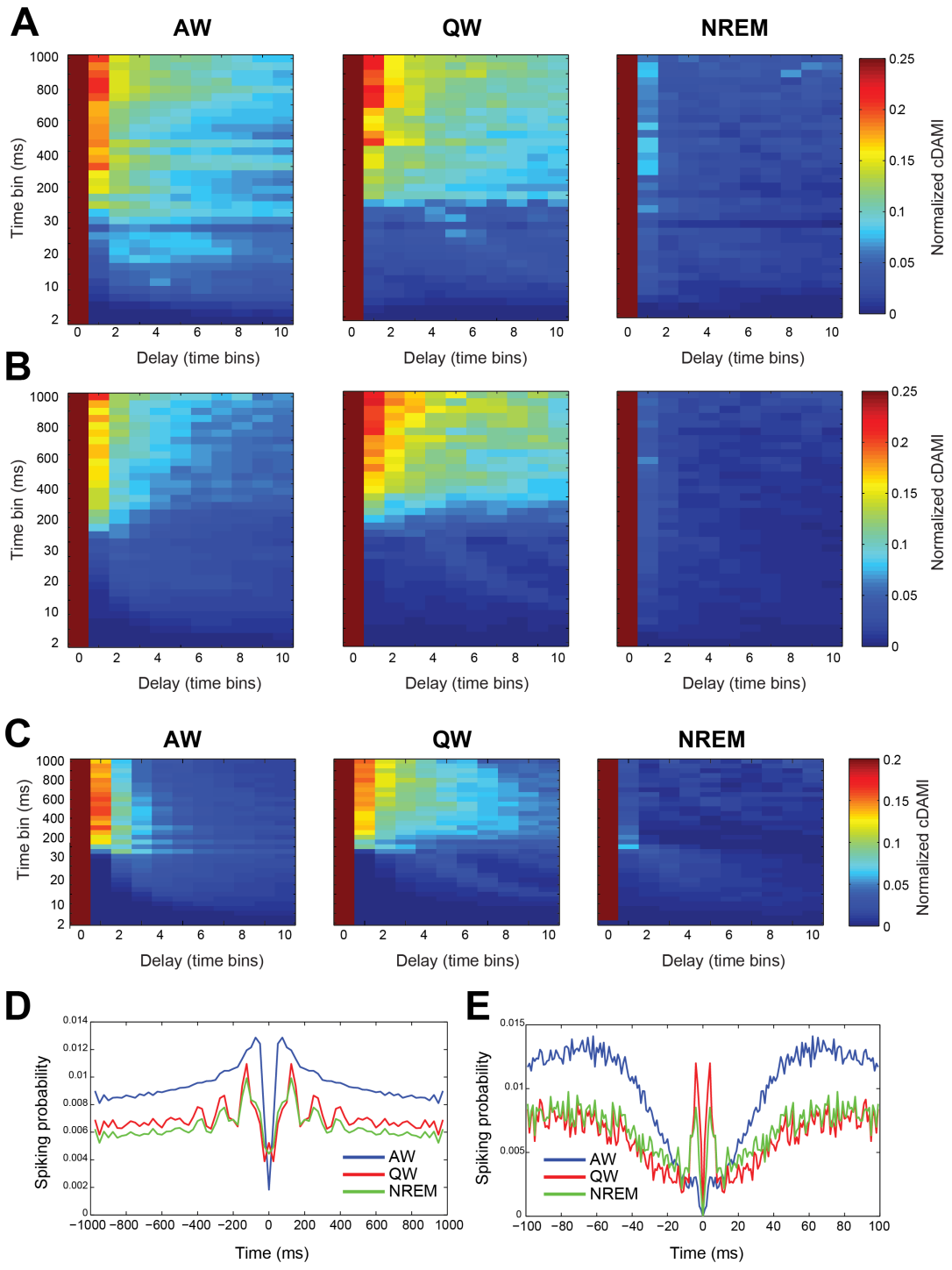

Figure R4 – Evaluation of cDAMI at different time scales. A. *Average values of cDAMI across neurons in the barrel cortex, computed using equispaced amplitude binning, for a single recording session. This panel shows the same data previously presented in Fig. 3A, without using interpolation, for temporal bins ranging from 2 ms to 1000 ms.* ***B.*** *Same as A, using equipopulated amplitude binning.* ***C.*** *Example cDAMI plot for a single example neuron.* ***D.*** *Auto-correlogram for the neuron shown in C, computed using a 25 ms bin, in the range -1 to 1 s.* ***E.*** *Same as D, computed using a 1 ms bin in the range -100 ms to 100 ms.*

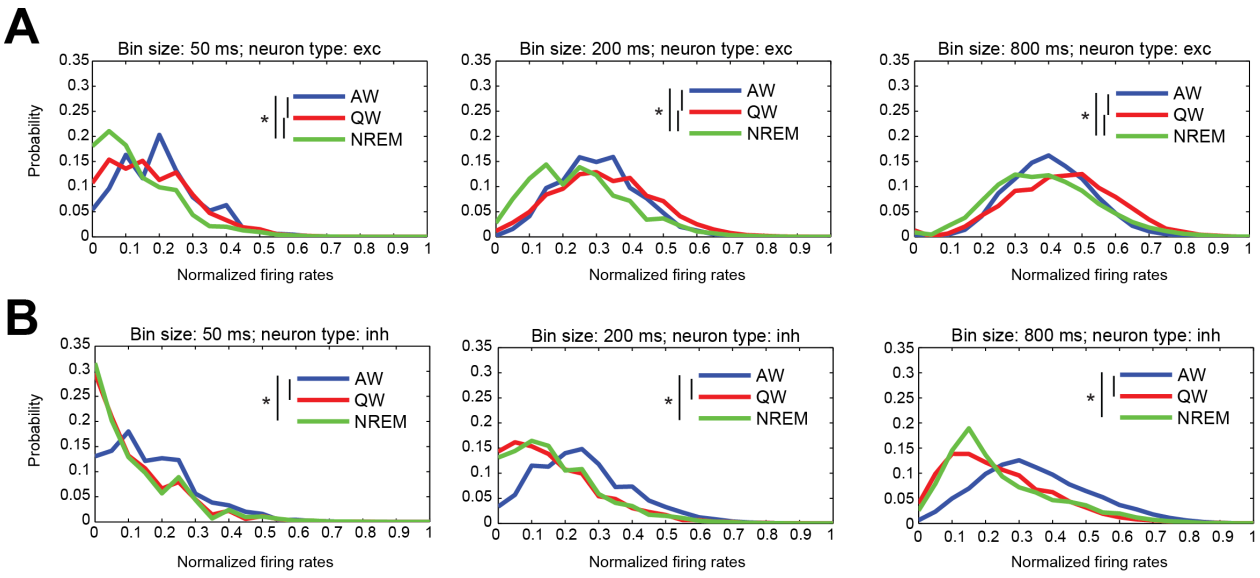

Figure R5 - Distribution of normalized firing rates across brain states. A. *Distribution of within-state normalized firing rates for excitatory neurons only, computed as a function of temporal bin size (left: 40 ms, middle: 200 ms, right: 800 ms) and across brain states (blue: AW, red: QW, green: NREM). Firing rates within each brain state have been normalized (independently for each neuron) to the highest value recorded in a given brain states.* ***B.*** *Same as A, for inhibitory neurons only. In all panels asterisks indicate significant differences between distributions (p<0.05, Wilcoxon rank sum test with post-hoc analysis.)*

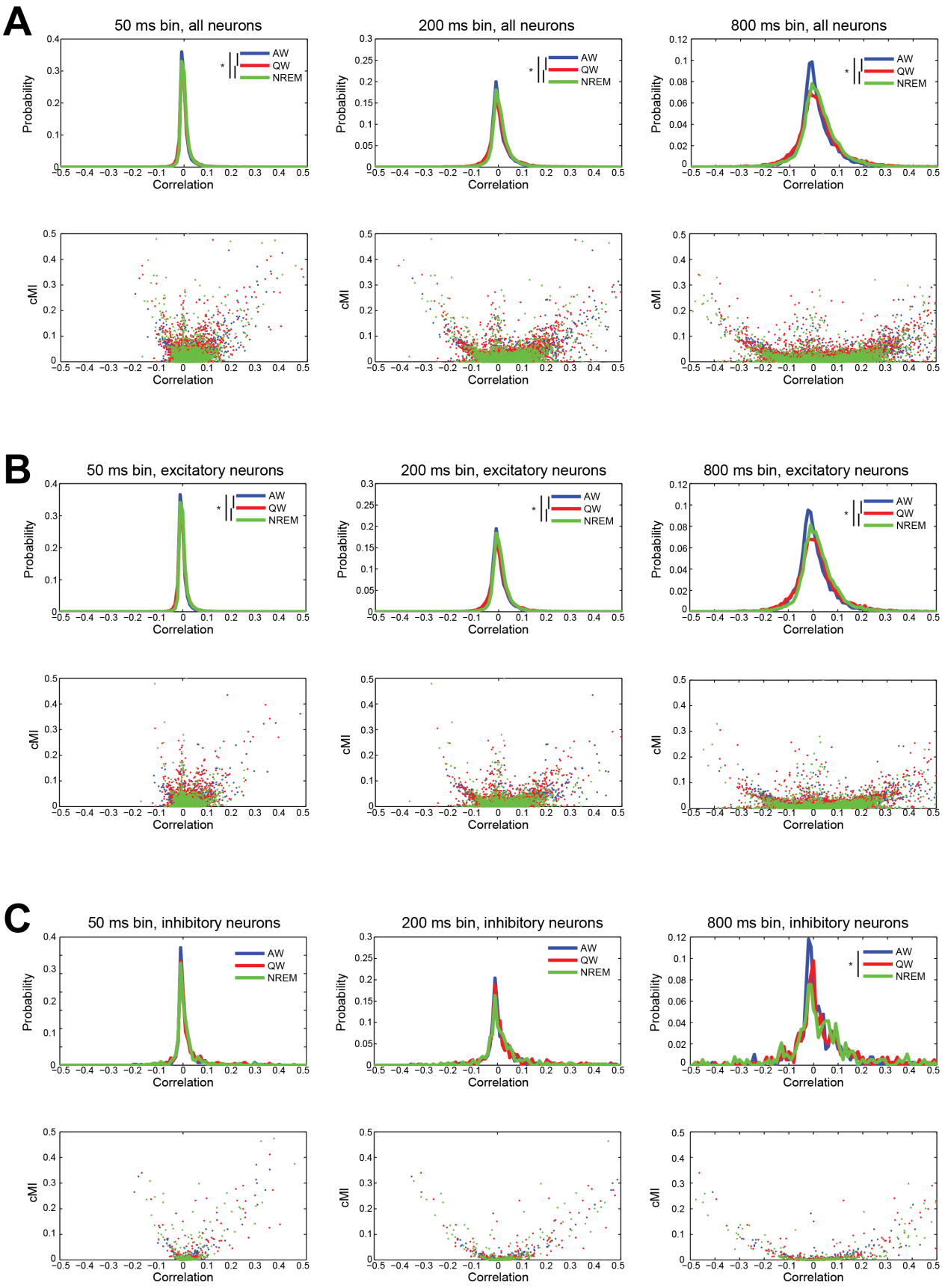
A
50 ms bin, all neurons
200 ms bin, all neurons
800 ms bin, all neurons
B
50 ms bin, excitatory neurons
200 ms bin, excitatory neurons
800 ms bin, excitatory neurons
C
50 ms bin, inhibitory neurons
200 ms bin, inhibitory neurons
800 ms bin, inhibitory neurons
AW
QW
NREM
Probability
cMI
Correlation

Figure R6 – Distribution of correlation values across brain states. A. *Top: Distribution of pairwise correlation values between firing rate trains, for all recorded neurons across brain states (blue: AW, red: QW, green: NREM). Firing rates were computed using three different time bins (left: 50 ms, middle: 200 ms, right: 800 ms). Bottom: Scatter plot showing the relationship between pairwise correlation values and cMI values. The same color convention used in the top panels apply here.* ***B.*** *Same as A, but only for pairs of excitatory neurons.* ***C.*** *Same as A, but only for pairs of inhibitory neurons. In the upper row of each panel, asterisks indicate significant differences between distributions (p<0.05, Kolmogorv-Smirnov test with post-hoc analysis).*

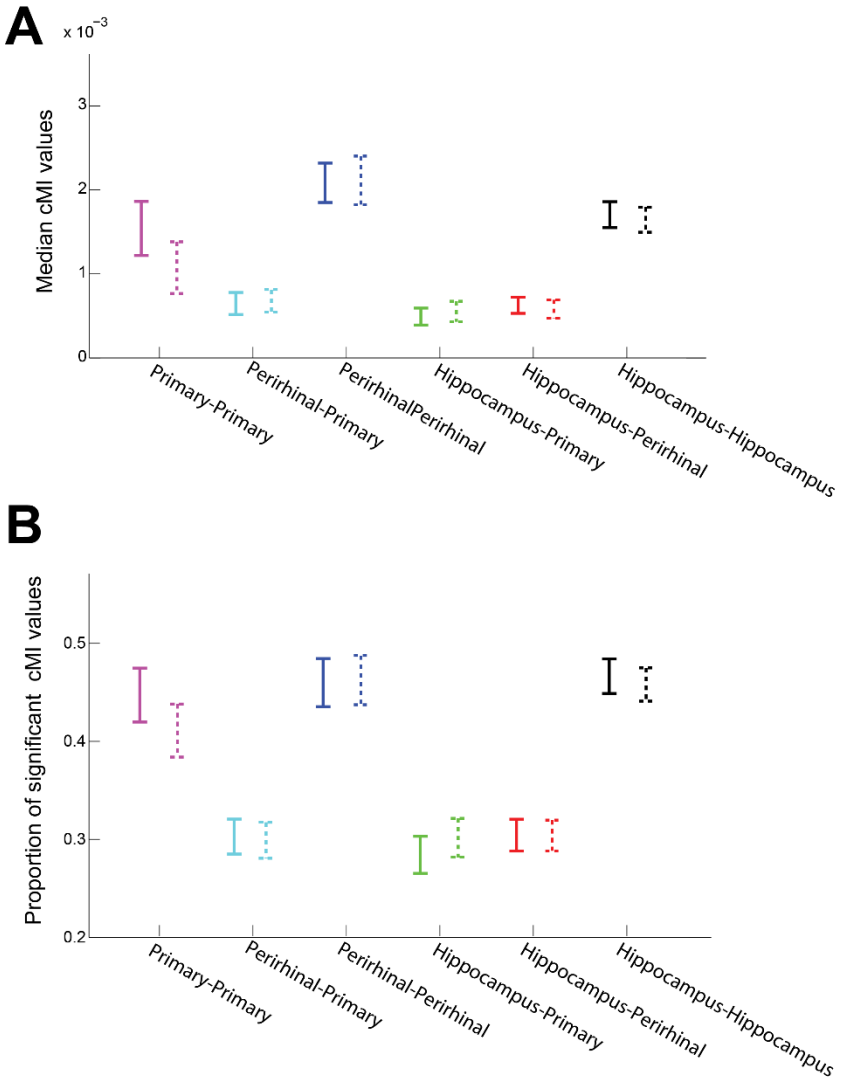

Figure R7 – Role of ripples in the estimation of cMI values. A. *Median cMI values (error bars: confidence intervals) during NREM for connections between different brain regions, computed either using whole NREM epochs (solid lines), or excluding time bins containing ripples (dashed lines).* ***B.*** *Same as A for the proportion of significant cMI values.*

Detection of Up and Down states

Up and down states were detected with a procedure similar to that shown in (Saleem et al., 2010).

Briefly, we filtered the LFP cortical signal (primary cortices cortex) in the slow wave and delta range (0.5-4.0 Hz), and then computed the instantaneous phase using the Hilbert transform. We then computed a normalized multi-unity activity (MUA) measure, by combining all spike trains from neurons isolated from the barrel cortex into a single, 1 ms bin, spike train. The resulting MUA trace was binarized (MUA:bin), to base the analysis of up/down states only on the presence/absence of action potentials (Vyazovskiy et al., 2009) and avoid giving too much weight to neurons with higher firing rates (e.g. interneurons). We then computed the circular histogram of MUA:bin firing rates as a function of phase of the low-passed filtered LFP (Fig. R8A). This plot shows a clear pattern, with some phases associated to stronger firing rate and vice versa. Note that, during to the binarization of firing rates, the differences between firing rates during up and down states can be reduced. Next, we computed the chance of an up state being observed as $L(t)=\cos(\phi(t)-\theta)$ (Saleem et al., 2010), where $\phi(t)$ is the instantaneous phase of the band-pass filtered LFP and θ is the phase corresponding to the peak in the firing rate (Fig. R8A). The distribution of L values (Fig. R8B) was then subdivided into three segments (corresponding to up states, down states and undetermined transition states) by using k-means clustering. Next, we verified the effectiveness of our algorithm by making the same plots shown in (Saleem et al., 2010): the occurrence of up and down states marked by colors on top of the filtered LFP (Fig. R8C) and the transition triggered LFP and MUA:bin averages (both for down-up transitions, see Fig. R8D, and up-down transitions, see Fig. R8E). It can be seen that these plots reliably mirror those shown in Fig. 7 of (Saleem et al., 2010), specifically as concerns the portion of each LFP trace that corresponds to an up or down state and – more importantly – the increase or decrease in MUA:bin firing rate following the transition to an up or down state, respectively. We only considered for the following analyses up and down states with a duration of at least 200 ms, in order to be able to employ cMI over valid time bins (see our response to previous points).

Importantly, the objective of our procedure was not to precisely identify the exact beginning and end of up and down states, but rather to have a reliable indicator of when up and down states occur. For this reason we implemented a simplified version of the algorithm presented in (Saleem et al., 2010). Also, by focusing on a single cortical portion (barrel cortex and primary visual cortex) we could now evaluate how coupling between neurons changes during up (down) states both locally and distally. Specifically, this enabled us to quantify what happened to the coupling between two areas when an up (or down) state was detected in a given region (i.e. primary cortices). This is of utmost relevance, since up and down states are not necessarily brain-wide events, and slow oscillations themselves are known not to be spatially homogeneous, but are rather travelling events (Compte et al., 2003; Massimini et al., 2004).

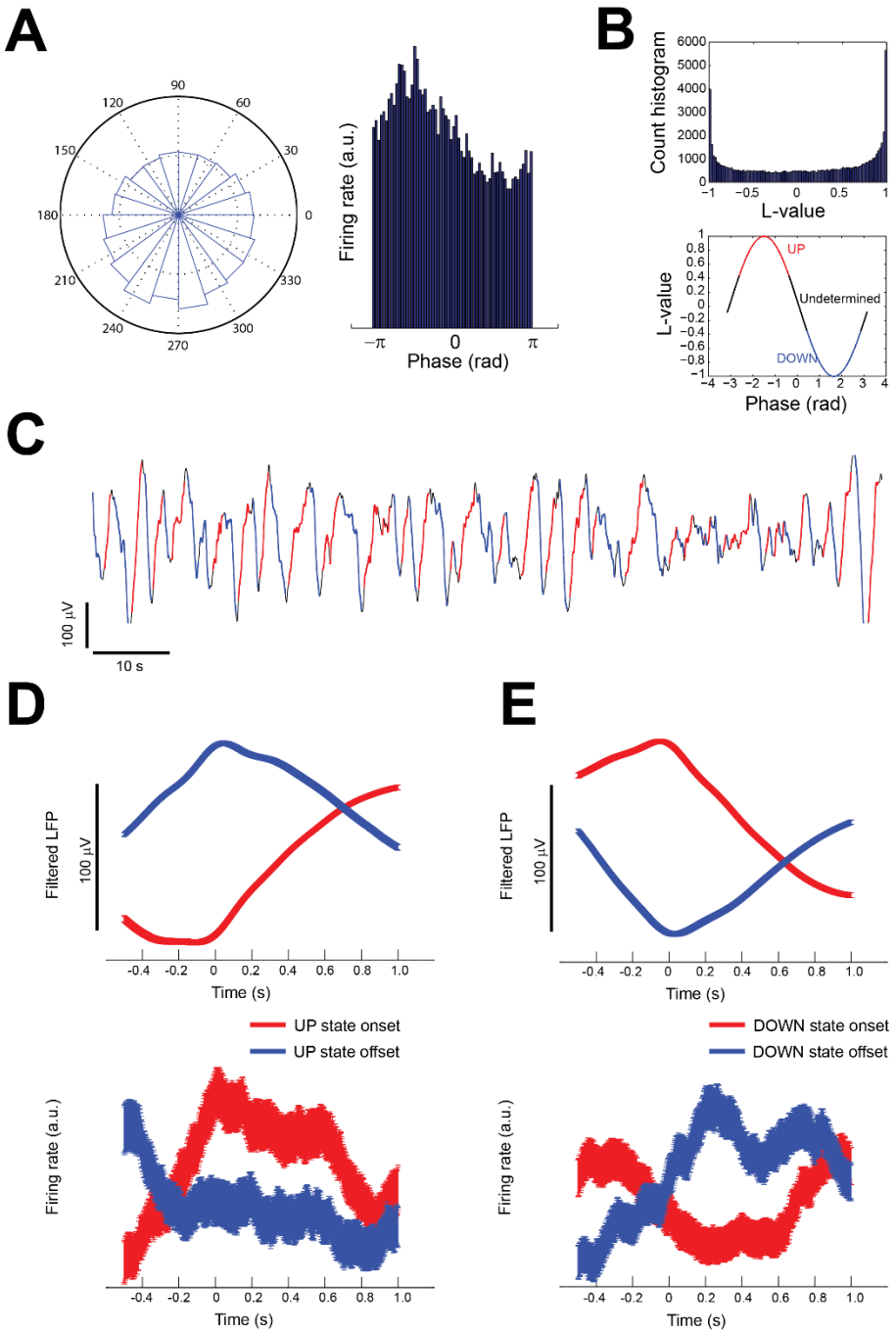

Figure R8 – Estimation of Up and Down states. A. *Left: Circular distribution of firing rate values in primary cortices (computed over MUA:bin traces) as a function of the instantaneous phase of band-pass filtered LFP signals, for an example recording session. Right: Same as the left panel, shown on a linear axis and with finer binning.* ***B.*** *Top: Histogram of L-values (chance of an up state being observed, see (Saleem et al., 2010)). Bottom: L-values as a function of the phase of the LFP signals. Colors indicate the output of the k-means clustering procedure. Red: phase interval corresponding to estimated up states. Blue: phase interval corresponding to estimated down states. Black: phase interval not corresponding to an up or a down state.* ***C.*** *Example filtered LFP segment during*

NREM sleep, with estimated up and down states indicated, respectively, in red and blue. ***D.*** *Top: Transition-triggered average LFP traces, aligned to the estimated onset and offset (t=0) of up states (red and blue traces, respectively). Bottom: same as top panel, for firing rates computed on the MUA:bin traces. All traces area mean ± SEM.* ***E.*** *Same as D, but for down state transitions (t=0).*

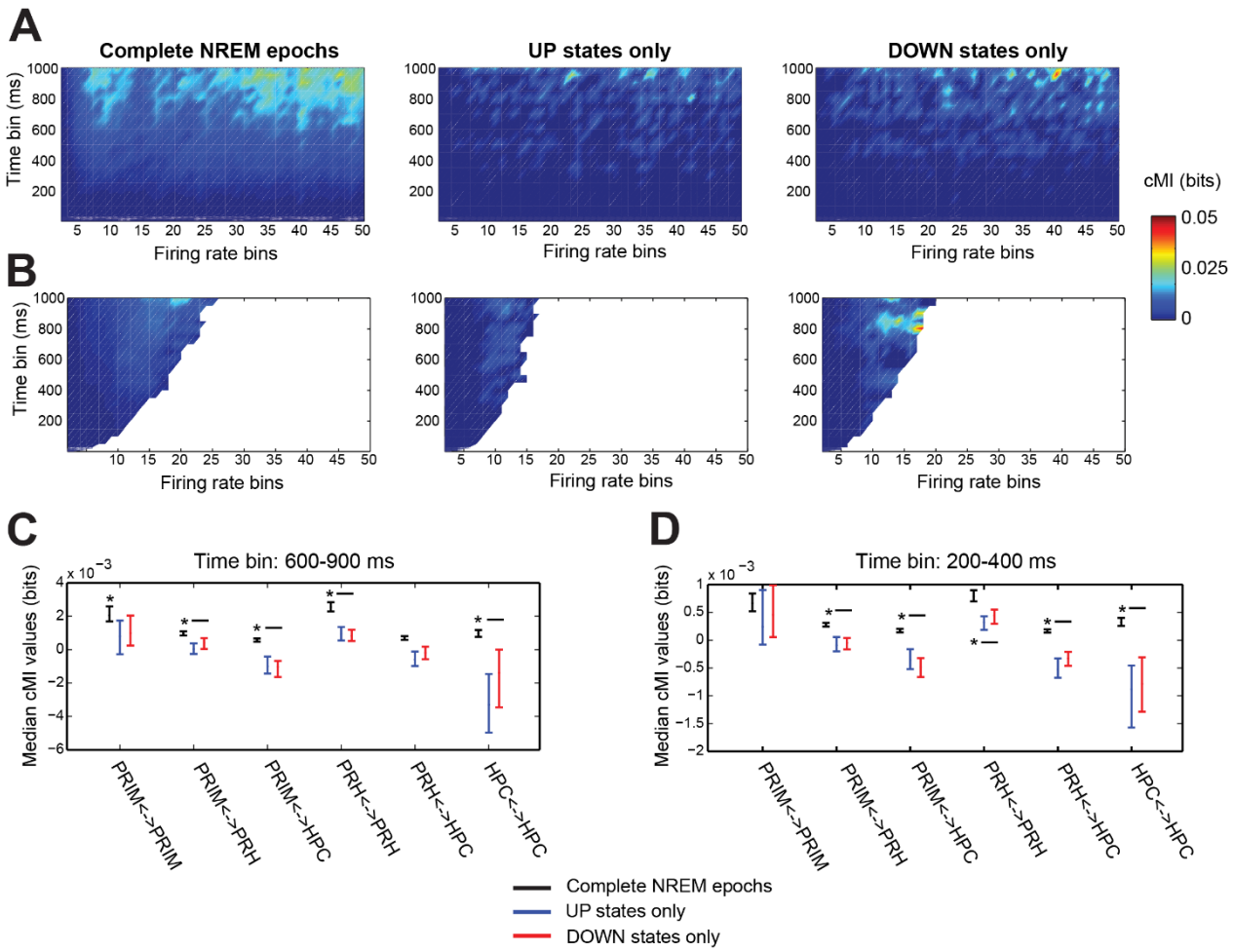

Figure R9 – cMI values for Up and Down states. A. *cMI values for an example pair of neurons, computed using equispaced amplitude binning, over complete NREM epochs (left), Up states only (middle) and Down states only (right). Notice the consistency of cMI values in the left column, compared to the "salt and pepper" appearance of the middle and right columns.* ***B.*** *Same as A, computed using equipopulated amplitude binning. C. Median cMI values in the 600-900 ms time range as a function of set of connections within or between brain areas, computed in NREM sleep using complete epochs (black), only Up states (blue) or only Down states (red). Black asterisks indicate values significantly different from zero (p<0.05, one-sided Wilcoxon test, whole epochs only, as no significant values were observe when considering only Up or Down states). Black lines indicates significant differences between cMI values computed over whole epochs, Up states only, or Down states only (p<0.05, Friedman test with post hoc analysis).* ***D.*** *Same as C, for the200-400 ms time range.*

Reference list

Compte A, Sanchez-Vives MV, McCormick DA, Wang X-J (2003) Cellular and network mechanisms of slow oscillatory activity (<1 Hz) and wave propagations in a cortical network model. J Neurophysiol 89:2707–2725.

Massimini M, Huber R, Ferrarelli F, Hill S, Tononi G (2004) The sleep slow oscillation as a traveling wave. J Neurosci 24:6862–6870.

Saleem AB, Chadderton P, Apergis-Schoute J, Harris KD, Schultz SR (2010) Methods for predicting cortical UP and DOWN states from the phase of deep layer local field potentials. J Comput Neurosci 29:49–62.

Vyazovskiy VV, Olcese U, Lazimy YM, Faraguna U, Esser SK, Williams JC, Cirelli C, Tononi G (2009) Cortical firing and sleep homeostasis. Neuron 63:865–878.